

New proton dynamics in solids revealed by vibrational spectroscopy with neutrons

F. Fillaux*

Lab Dynamique, Interactions et Reactivité, Gr. des Lab. de Vitry-Thiisis, LADIR-CNRS, 2 Rue Henry-Dunant, 94320 Thiais Cedex, France

Received 24 October 1998; accepted 15 November 1998

Abstract

Recent studies with the incoherent inelastic neutron scattering (INS) technique of proton dynamics in various solids are reviewed. Simulation of spectral intensities reveal that vibrational dynamics for protons are better represented with localised modes, rather than with conventional normal modes. Tunnelling transitions are observed for proton transfer along hydrogen bonds in various systems, either ionic in nature, like KHCO_3 , or molecular, like polyglycines. The phonon assisted tunnelling model is not confirmed. Free recoiling entities with proton mass have been observed in different solid-state protonic conductors. Electric charges of these entities and interaction with electrons of the host lattice are tentatively related to protonic and electronic conductivity. New protonic species have been characterised. In $\gamma\text{-MnO}_2$, charge-compensating protons in Mn^{4+} vacancies form $(\text{H}^+)_4$ entities, with tetrahedral structure, rotating freely inside oxygen octahedra. In β -alumina, protonic entities are amenable to tetrahedral structures instead of the trigonal structure anticipated for oxonium ions. © 1999 Elsevier Science B.V. All rights reserved.

Keywords: Inelastic neutron scattering; Vibrational spectroscopy; Free protons; Manganese dioxides; Coals; Graphite intercalation compounds; Polyanilines; β -alumina

1. Introduction

A detailed view of proton dynamics in solids is of primary importance for a better understanding of the complex relationship between chemical composition, structure, and proton mobility in materials (proton transfer, phase transitions, proton conductivity, etc.) [1–7]. These dynamics are observed over a very broad range of time scales with various experimental techniques: diffraction, NMR, NQR, quasi-elastic neutron scattering (QENS), vibrational spectroscopy, etc.

Protons moving fast play a key role in proton transfer and transport processes. They are best

observed with vibrational spectroscopy techniques on a time-scale shorter than 10^{-10} s. The infrared and Raman techniques frequently used in fundamental and applied research on materials suffer from limitations due to the nature of the interaction of photons with matter. Most of these limitations are irrelevant if neutrons instead of photons are used to perform incoherent inelastic neutron scattering (INS) experiments.

1.1. Intensities

For optical techniques, intensities are related to the derivatives of either the dipole moment in the infrared, or the polarizability tensor in Raman. These quantities, which are very sensitive to the hybridisation state of valence electrons, are largely

* Tel.: + 33-1-49-781283; fax: + 33-1-49-781323.

E-mail address: fillaux@glvt-cnrs.fr (F. Fillaux)

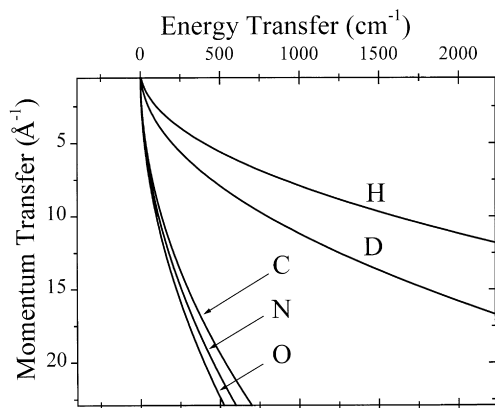


Fig. 1. Recoil lines in (Q, ω) space for free particles.

unknown. They cannot be measured directly and quantum calculations are not yet able to provide reliable values. Therefore, measured intensities cannot be fully exploited. With INS, the neutron scattering process is entirely attributable to nuclear interactions and cross-sections are independent of chemical bonding. Transition moments can be calculated accurately and directly compared to measured intensities. In addition, there is no symmetry related selection rule.

1.2. Contrast

Because the proton cross-section for INS is one order of magnitude greater than that for any other atom, proton dynamics can be studied in many different non-hydrogenous environments, even for rather low concentrations in protonic species. This proton selectivity can be further exploited because the deuterium atom (^2H or D) has a very much smaller cross-section than the proton. For a system with several protons, specific deuteration of some sites therefore simplifies the observed signals. As a result, INS intensities provide information on proton dynamics that can be analysed with greater confidence than the corresponding infrared and Raman spectra.

1.3. Momentum transfer

INS spectroscopy offers the unique opportunity to measure vibrational spectra over a broad range of energy and momentum transfer ($\mathbf{Q} = \mathbf{k}_i - \mathbf{k}_f$ with wave-vector amplitudes $|\mathbf{k}_i| = 2\pi/\lambda_i$ and $|\mathbf{k}_f| = 2\pi/\lambda_f$,

where λ_i and λ_f are the incident and scattered wavelengths, respectively). The intensity for incoherent scattering by protons can be represented with the scattering function [8]

$$S(\mathbf{Q}, \omega) = |\langle \Psi_f(\mathbf{r}) | \exp(i\mathbf{Q}\mathbf{r}) | \Psi_i(\mathbf{r}) \rangle|^2 \delta(E_{if} - \hbar\omega), \quad (1)$$

$\Psi_i(\mathbf{r})$ and $\Psi_f(\mathbf{r})$ are the wave functions, in the initial and final states, respectively, depending on the spatial coordinate \mathbf{r} . E_{if} is the energy of transition and $\hbar\omega$ is the neutron energy transfer. For each vibrational mode, the INS spectral profile in \mathbf{Q} is the Fourier transform of the self-correlation function $|\Psi_i \Psi_f|$ that contains spatial information on the wave functions. For optical techniques $\mathbf{Q} \approx 0$.

1.4. Free particles

For free particles with mass M , energy transferred from neutrons is totally converted into kinetic energy according to $E = \hbar^2 Q^2 / 2M$ ($\sim 16Q^2/M$ with E , Q and M in cm^{-1} , \AA^{-1} and amu, respectively). Free particles give a continuum of intensity that is a maximum in (Q, ω) space along the “recoil” line for mass M (Fig. 1). It is of great importance to stress that free particles (e.g., protons) cannot be directly observed with optical techniques.

1.5. Penetration depth

In many materials, photons are strongly absorbed or refracted over wide frequency ranges. Only an extremely thin layer at the surface can be observed. In contrast to this, neutrons can penetrate most media and probe proton dynamics in the bulk.

With the MARI spectrometer at the ISIS pulsed neutron source (Rutherford Appleton laboratory, Chilton, UK) we can measure the scattering function over large domains of energy and momentum transfer to obtain detailed information on proton dynamics. With the TFXA spectrometer, only the narrow slice of (Q, ω) space along the recoil line for mass 1 amu (Fig. 1) is probed. This corresponds to the maximum intensity for proton oscillators. Measurements are easier and faster than when using the MARI instrument but the TFXA spectrometer provides less information.

Vibrational spectroscopy with neutrons already has achieved interesting results in most of the classic

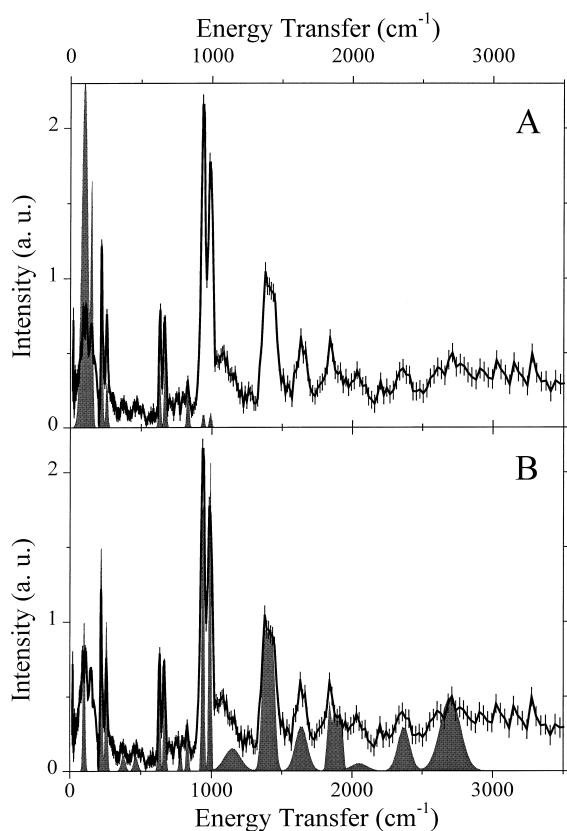


Fig. 2. Comparison of the observed (error bars) and calculated (dark) INS spectra of KHCO_3 at 20 K. (A) normal modes; (B) localised modes, after Ref. [21].

disciplines of physics, chemistry and biology. INS appears more and more complementary to optical techniques. New results obtained with INS provide a better understanding of infrared and Raman spectroscopies and consequently lead to a more effective use of these techniques. However, the INS technique is rather novel. It can be used only at a very limited number of places and requires quite large amounts of samples (typically several grams). Consequently, the number of problems which has been tackled so far is still rather modest compared to the huge amount of knowledge accumulated over several decades with infrared and Raman techniques.

In this paper, the main impacts of INS on force-field calculations, quantum proton transfer along hydrogen bonds and recent evidence for free protonic entities, or new protonic species are presented. These results

open up further prospects for new concepts that could be relevant for the tailoring of new materials.

2. Force-fields calculations: normal versus localised modes

It is widely accepted that vibrational dynamics of atoms and molecules are reasonably well represented with harmonic force fields. The resolution of the secular equation transforms a set of (say N) coupled oscillator into (N) independent oscillators along orthogonal (normal) coordinates. Eigenvalues of the dynamical matrix are normal frequencies and eigenvectors give atomic displacements for each normal mode [9–14]. If band intensities cannot be fully exploited, these vectors are unknown and force fields refined with respect to observed frequencies only are largely under-determined. For complex systems, symmetry consideration or/and isotopic substitutions may remove only partially this under-determination.

With the INS technique, force fields can be refined with respect to the full spectral profiles including both frequencies and intensities [15–20]. This technique is most powerful for hydrogenous samples for which intensities are dominated by modes involving large proton displacements. However, contributions from other atoms are difficult to estimate precisely and can be easily ignored.

When harmonic force fields are used to represent local atom–atom interactions in molecular crystals, the mean positions of the protons that oscillate at high frequencies (internal modes) follow the slow lattice vibrations adiabatically. This proton riding effect should give rise to large intensities for lattice modes at low frequency. Moreover, intensities for internal molecular vibrations should be depressed dramatically by an exponential term referred to as the Debye–Waller factor, $\exp[-\langle(\mathbf{Q}\cdot\mathbf{u})^2\rangle]$, where \mathbf{u} is the displacement vector for atoms and $\langle\rangle$ means averaged over the density of states. Consequently, it has been speculated that internal modes at a high frequency (say above $\sim 1000\text{ cm}^{-1}$) and momentum transfer values should be almost invisible with INS. However, this is largely in error. For example, CH stretching modes were observed at $\sim 3000\text{ cm}^{-1}$ and the role of the Debye–Waller factor had to be reconsidered.

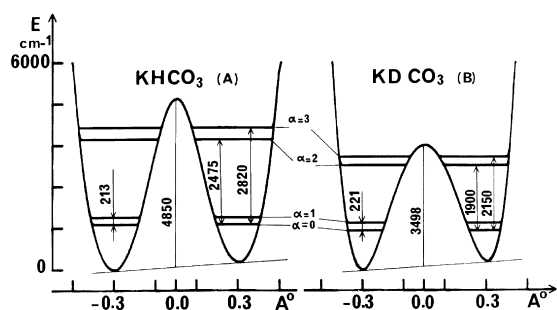


Fig. 3. Double minimum potential functions for proton (deuteron) transfer dynamics derived from the infrared and Raman band shape analysis of the OH (OD) stretching modes in KHCO_3 (KDCO_3) crystals, after Ref. [33].

It has been shown recently that the INS spectrum of potassium hydrogen carbonate (KHCO_3) cannot be represented with conventional harmonic force fields [21]. The observed intensities for lattice modes are smaller than the calculated ones by at least one order of magnitude (Fig. 2(A)). It was concluded that there is virtually no riding effect. Protons are almost totally decoupled from the surrounding heavy atoms and their dynamics are better represented with localised modes in a “fixed” (laboratory) referential frame (Fig. 2(B)). From the standpoint of the INS technique, KHCO_3 can be regarded as a crystal of protons so weakly coupled to the surrounding atoms that the framework of carbonate and potassium ions can be virtually ignored. Dynamical models are thus greatly simplified. Besides, this view is not specific to the ionic nature of the crystal. Similar conclusions were obtained with a molecular crystal (the *N*-methylacetamide molecule [22], see below Fig. 5) and a polymer (polyglycine [23], see below). These results severely undermine the representation of vibrational spectra with usual normal modes. However, the phenomenological approach proposed so far lacks contact with physics. It has been recently suggested that the peculiar proton dynamics could be a consequence of the non-local nature of quantum mechanics [24].

3. Proton transfer

Another highlight of the INS technique concerns proton transfer along pre-existing hydrogen bonds [25].

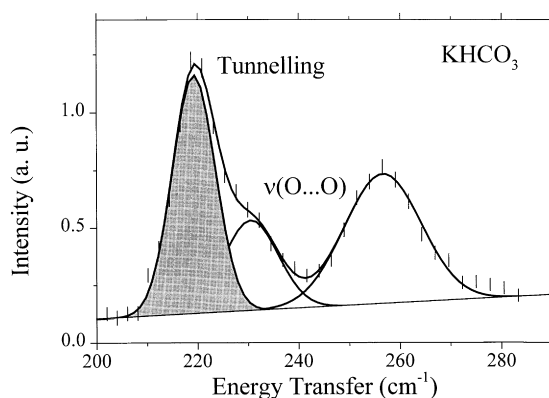


Fig. 4. The INS spectrum of KHCO_3 at 20 K in the proton tunnelling region, after Ref. [21].

3.1. Potassium hydrogen carbonate

KHCO_3 is a prototypical system for proton transfer dynamics. The crystal contains centro-symmetric dimer entities $(\text{HCO}_3^-)_2$ and this structure remains unchanged from 298 to 98 K [26,27]. (We are not aware of any diffraction work at a lower temperature.) The hydrogen bond with length $\text{O}\cdots\text{O} = 2.59 \text{ \AA}$ (2.61 \AA for KDCO_3) is moderately strong. At 298 K protons are disordered between two sites located at $\sim \pm 0.3 \text{ \AA}$ off-centre of the hydrogen bond, with a population ratio of $\sim 1:4$. However, diffraction studies cannot distinguish statistical and dynamical disorders easily.

The OH-stretching vibration of KHCO_3 is of particular interest as quantum proton transfer (tunnelling) is best observed for vibrations along the reaction path. In the infrared and Raman spectroscopies this mode gives broad bands, with several sub-maxima between 1800 and 3500 cm^{-1} [28–30]. Although various models have been proposed for hydrogen bond dynamics, and extensive quantum-mechanical calculations have been performed [31,32], a detailed understanding of the band shaping mechanism is still lacking. In spite of these limitations, a quasi-symmetric double minimum potential along the proton stretching mode coordinate was proposed (Fig. 3) [33]. The “tunnelling” transition associated with quantum transfer of a single proton was calculated at 213 cm^{-1} . Thanks to the great sensitivity of the INS technique to proton displacements with large amplitudes, this transition was observed at 216 cm^{-1} ,

close to the O···O stretching bands (Fig. 4) [21]. The dynamical nature of the proton disorder was thus established.

Surprisingly, the “tunnelling” band is rather sharp. The measured full width at half maximum of $\sim 10 \text{ cm}^{-1}$ is probably greater than the real bandwidth. On the one hand, this confirms that proton transfer is totally decoupled from heavy atom dynamics, in line with the remainder of the spectrum. On the other hand, this is in contrast to the “phonon assisted tunnelling” model [34] that supposes a large modulation of the double minimum potential by (O···O) low frequency modes. Tunnelling transitions observed in various hydrogen bonds are quite similar [35–37]. These potentials correspond to the local transfer of a single proton. Clearly, the opportunity to observe tunnelling transitions with INS is an important step towards a better understanding of proton transfer dynamics. Further improvements in the spectrometer resolution should allow us to analyse tunnelling band shapes in more details.

3.2. Proton transfer in amides and polypeptides

The *N*-methylacetamide molecule ($\text{CH}_3\text{CONHCH}_3$) and polyglycine ($(-\text{CO}-\text{CH}_2-\text{NH}-)_n$) are simple models for the peptide unit, which is of central importance to many biological structures and processes. The heavy atom skeleton of this unit (C, O and N) is almost planar, with the CO and NH bonds *trans* to each other across the central CN bond [38,39]. Resonance between two mesomeric forms, namely amide-like ($\text{O}=\text{C}-\text{N}-\text{H}$) and imidol-like ($\text{O}^--\text{C}=\text{N}-\text{H}^+$), was proposed by Pauling [39] with the amide-like form being dominant. In the crystalline state, the NH group of one molecule links to the CO group of a neighbour to create infinite chains of hydrogen-bonded $\text{NH}\cdots\text{O}$ bridges, with $\text{N}\cdots\text{O}$ distances of $\sim 2.8 \text{ \AA}$, which are similar to those observed for proteins. In the solid state, polyglycine may adopt two secondary structures: the antiparallel chain rippled-sheet (I) [40] and the triple helix, collagen-like form (II) [41].

INS spectra of partially deuterated analogues $\text{CD}_3\text{CONHCD}_3$ and $(-\text{CO}-\text{CD}_2-\text{NH}-)_n$ have been studied to investigate proton dynamics in hydrogen bonds. Surprisingly, force-field calculations of INS intensities confirm most of the conclusions previously

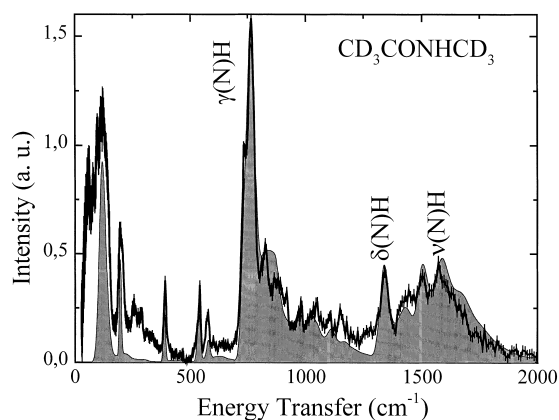


Fig. 5. Comparison of the observed (with error bars) and calculated (dark) INS spectra of the partially deuterated *N*-methylacetamide molecule ($\text{CD}_3\text{CONHCD}_3$) at 20 K, after Ref. [22]. The proton dynamics is virtually decoupled from the heavy atoms and the proposed assignment scheme is shown.

obtained for hydrogen-bonded dimers in ionic crystals, although these systems are molecular in nature (Fig. 5) [22,23]. Proton dynamics are largely isolated from the molecular backbones. Besides, in addition to the proton bending modes at $\sim 770 \text{ cm}^{-1}$ (out-of-plane) and $\sim 1330 \text{ cm}^{-1}$ (in plane) and their overtones and combinations, a band is observed at 1575 cm^{-1} with a rather large INS intensity corresponding to that anticipated for a pure proton mode. This band is not compatible with previous assignment schemes and must be logically regarded as the NH stretching mode (Fig. 5). Therefore, the previous estimate for the vibrational frequency of this mode ($\sim 3000 \text{ cm}^{-1}$), based on the optical techniques, is higher by almost a factor of 2. This new assignment scheme was further confirmed with neutron Compton scattering measurement [42]. Consequently, the infrared and Raman spectra were re-assigned.

These results are obviously in contrast to the normally accepted view and imply a significant weakening of the covalent bond between the N and H atoms compared to what was thought previously. Instead of the covalent representation of the hydrogen bond ($\text{NH}\cdots\text{O}$), the ionic model ($\text{N}^{\delta-}\cdots\text{H}^+\cdots\text{O}^{\delta-}$) appears to be more realistic with regard to the low frequency and large intensity in the infrared of the proton stretching mode.

In order to get an insight into proton dynamics at

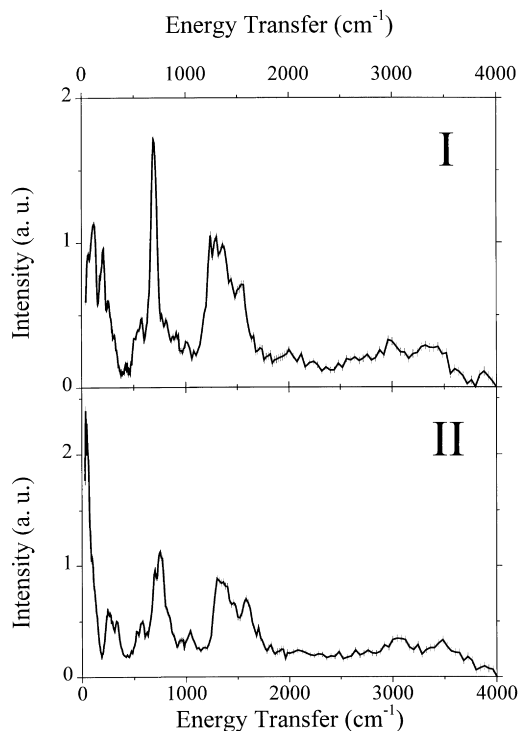


Fig. 6. INS spectra of the partially deuterated polyglycines ($-\text{CO}-\text{CD}_2-\text{NH}-$)_n I (top) and II (bottom) at 20 K.

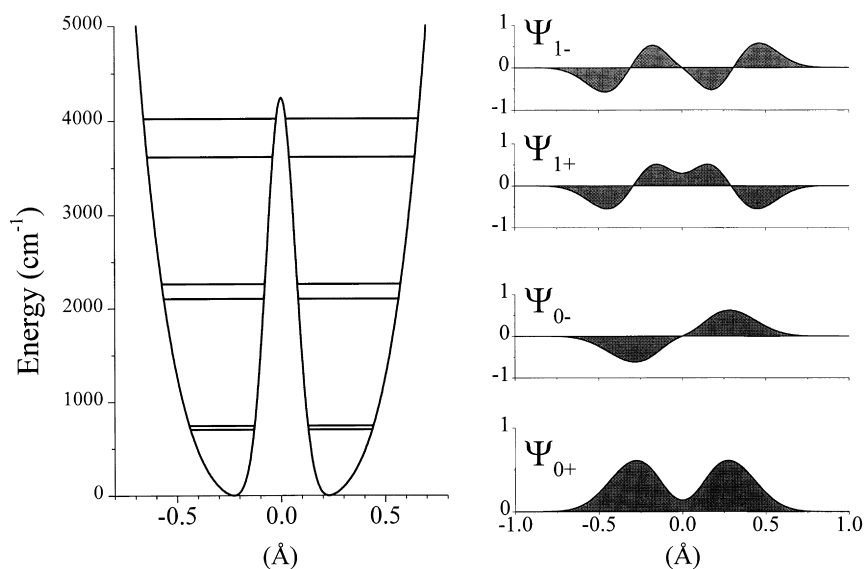
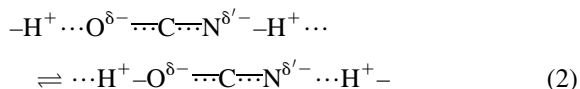


Fig. 7. Symmetric double minimum potential for the stretching proton mode of polyglycine II: $V = 21\,623x^4 + 4323 \exp(-101x^2)$ V and x are in cm^{-1} and \AA units, respectively.

room temperature, it is necessary to measure temperature effects. Unfortunately, INS spectra are best observed at low temperatures where contributions of phonon wings are a minimum. The infrared and Raman techniques can be used more routinely to observe temperature effects. All spectra are amenable to the new assignment scheme where the proton stretching modes are in the $1500\text{--}1600\text{ cm}^{-1}$ region and the overtones between 2900 and 3300 cm^{-1} . Similar conclusions have been drawn from the spectra of polyglycine I and II [22]. However, in contrast to the case of *N*-methylacetamide, dynamics are almost insensitive to temperature effects.

According to the new assignment scheme for amides and polypeptides, the proton stretching modes split into two components in the fundamental and overtones region with relative intensities changing dramatically with temperature in the case of *N*-methylacetamide. At first sight, this can be interpreted along two different lines. First, the two components for each mode may correspond to a thermal equilibrium between amide-like and imidol-like forms which are schematically represented as



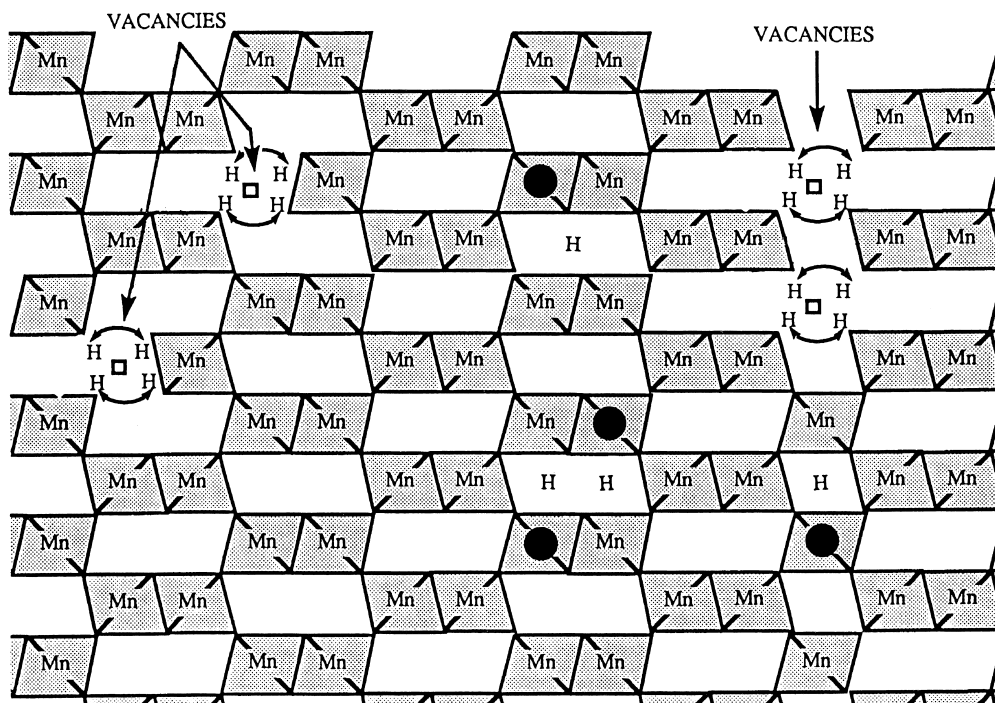


Fig. 8. Schematic view of the model structure proposed by Ruetschi [47] for nsutite. ●: Mn(III) defects.

The two forms should be almost equiprobable at room temperature whilst only one of them dominates at 20 K.

An alternative interpretation is a double minimum potential, close to symmetry, along the hydrogen bond and tunnel splitting. The infrared and Raman spectra are amenable to this model [21,22]. However, because a multitude of effects control intensities in these spectroscopies, it is impossible to characterise the double minimum unambiguously. The most convincing evidence for the symmetric double minimum potential is to observe the tunnelling transition at low frequency corresponding to the removal of the ground state degeneracy. Only the INS technique can provide this information.

INS spectra of the partially deuterated polyglycine I and II are quite similar, apart from a very intense band at $\sim 40 \text{ cm}^{-1}$ for polyglycine II which has no counterpart for polyglycine I (Fig. 6). Because of the great sensitivity of INS to proton displacements, this band should correspond to proton tunnelling. This is confirmed by the $S(Q, \omega)$ map of intensity obtained with the MARI spectrometer at ISIS (Rutherford

Appleton Laboratory) [43]. The large intensity and the Q dependence of the signal at $\sim 40 \text{ cm}^{-1}$ are not amenable to any vibrational mode of the chains. In contrast, the Q profile corresponds to that anticipated for a symmetric double minimum potential with two minima separated by $\sim 0.5 \text{ \AA}$. The potential function consistent with the observed spectra has a barrier height of 4230 cm^{-1} (Fig. 7). In this case, amide-like and imidol-like forms cannot be distinguished as the proton is delocalized. Proton transfer occurs at any temperature as a direct consequence of the hydrogen bond formation.

The symmetric double minimum potential for polyglycine II is in conflict with intuitive ideas about proton transfer. Double minimum potentials close to symmetry are anticipated for rather strong and symmetrical hydrogen bonds, whilst hydrogen bonds between amides and peptides are normally regarded as moderately strong and, obviously, non-symmetric. Another remarkable aspect of proton tunnelling in polyglycine II is that there is no evidence for collective effects. Consequently, proton tunnelling is purely a local dynamics.

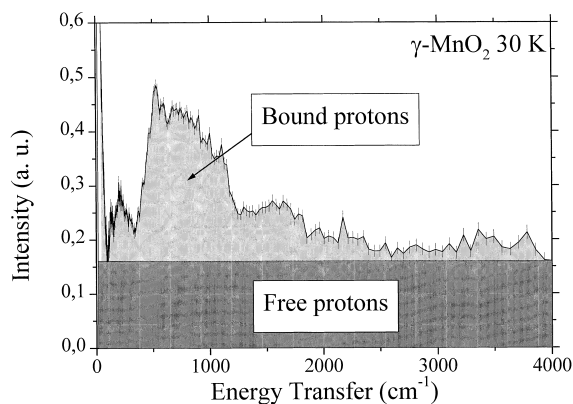


Fig. 9. INS spectrum of nsutite along the recoil line for mass 1 amu measured with the TFXA spectrometer, after Ref. [46].

The main limitation of vibrational spectroscopy is that it does not provide any information on the proton location along the hydrogen bond and we are not aware of any diffraction work confirming the double minimum potential for amides or peptides. In contrast to this, recent neutron diffraction work on acetanilide do not provide any evidence for proton delocalisation along the hydrogen bond [44,45]. This apparent conflict is one of the most fascinating challenges. Further measurements with complementary techniques are necessary.

4. Free protons

The existence of free protons in solids has long

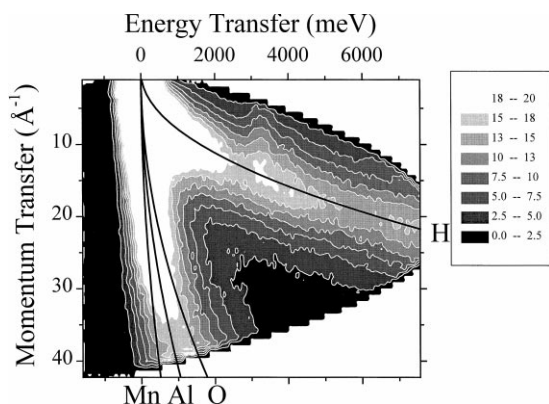


Fig. 10. Iso-contour map of intensity of $S(Q, \omega)$ for nsutite at 30 K, after Ref. [48]. The recoil lines for various nuclei are superimposed.

been regarded as unlikely, owing to the high chemical reactivity of this atom. In addition, free protons cannot be observed with the infrared and Raman techniques and cannot be characterised unambiguously with diffraction, NMR or QENS. Evidences for free protons obtained with the INS technique raise fundamental problems in solid-state physics. Are these free protons real charge carriers in proton conductors? Do they form energy bands similar to electrons? How do free protons correlate with the electronic structure of the host?

Free protons were first reported for nsutite (γ - MnO_2), a material commonly used for electrodes in alkaline batteries [46]. This electrochemically active material is an intergrowth of pyrolusite and ramsdellite structures, composed of oxygen octahedra (Fig. 8). It contains structural defects, mainly Mn(III) atoms, Mn^{4+} vacancies and protons [47]. It has been suggested that protons are either associated to defects or form structural water. However, the size of the water molecule is much greater than the structural channels and it has been supposed that protons should be more likely bound to oxygen atoms in the structure.

The INS technique provides the clearest view of proton dynamics as scattering cross-sections for Mn and O atoms are negligible. Two different types of protons can be distinguished in the TFXA spectrum along the proton recoil line in (Q, ω) space (Fig. 9).

- Protons bound to oxygen atoms, either in the bulk or at the surface give a broad band between 500 and 1000 cm^{-1} (and an overtone between 1000 and 2000 cm^{-1}). These bands correspond to libration of water molecules and surface OH groups.
- Free protons give the continuum intensity, underneath the bands, extending itself over the whole spectral range (and beyond 4000 cm^{-1}). These protons scatter neutrons at any energy transfer because they are not chemically bound to any atom. There is no visible intensity cut-off at low frequency. Therefore, the binding energy is negligible ($<20 \text{ cm}^{-1}/30 \text{ K}$) and protons are totally free, even at low temperature.

Because the neutron has no electric charge, it is not possible to distinguish H^+ , H^0 , H^- or any intermediate entity. Therefore, “free protons” refer to the scattering process by nuclei, rather than to effective electric charges.

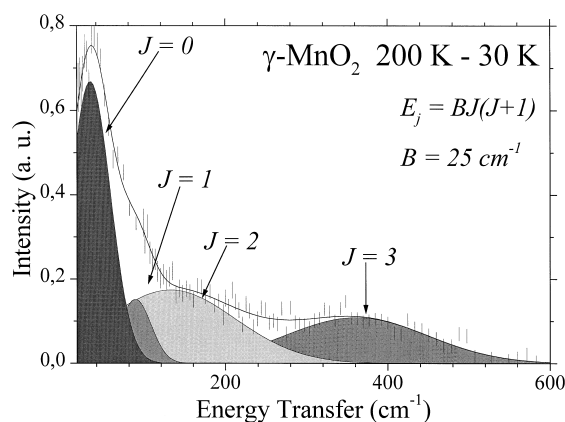


Fig. 11. INS difference spectrum for nsutite at 200 and 30 K. B is the rotational constant of the spherical top and J is the rotational quantum number.

Free protons in solids, like electrons, should give rise to energy band structures. However, the proton density (0.08 proton per MnO_2 entity) and thus the Fermi energy ($\sim 0.4 \text{ meV}/3 \text{ cm}^{-1}/4 \text{ K}$) are very low and quantum statistics for fermion gas cannot be observed.

The full scattering function $S(Q, \omega)$ gives a more detailed view of the free proton dynamics (Fig. 10) [48]. The maximum of the continuum intensity closely follows the “recoil line” for free particles with mass 1 amu. In principle, the width of the recoil signal should be determined by the distribution of kinetic momentum for free protons. For an isolated ideal gas at 30 K the width should be $\sim 0.4 \text{ \AA}^{-1}$. However, the observed width is more than one order of magnitude greater and corresponds to an effective temperature of $\sim 800 \text{ K}$. This broadening is related to the zero-point energy of the host matrix and can be compared to the Doppler effect. The observed width is the convolution of the kinetic momentum distribution for protons (very narrow) with that for the lattice density-of-states [48]. In accord with the theory, the continuum intensity is a constant along the recoil line and the width is half that of the elastic peak.

Free protons have been observed in various manganese dioxides, including lamellar ($\delta\text{-MnO}_2$) and Bi doped analogues [49–52]. All these materials are electrochemically active. In contrast, there is no evidence for free protons in the non-electrochemically active ramsdellite or groutite variety.

Free protons have been observed in various coal

samples [53–55] and $S(Q, \omega)$ maps of intensity are very similar to that presented before for nsutite. The recoiling particles are protons and the distribution of kinetic momentum is broadened by the lattice density-of-states. There is no evidence for molecular hydrogen (H_2), despite the great sensitivity of the INS technique. Free protons have also been reported in some carbon blacks [56].

In the graphite–nitric acid intercalation compounds G-HNO_3 ($\text{C}_{15}\text{HNO}_3$) the carbon hexagonal network behaves as a macrocation. These materials are good p-type conductors and can be regarded as “synthetic metals”. The INS spectra of the α form third stage at 30 K (F. Fillaux et al., unpublished) revealed the continuum of intensity anticipated for the recoil of free protons. According to the ratio of free to bound protons ($\sim 1:3$) the intercalated species correspond to oligomer-like entities $(\text{NO}_3\text{HNO}_3\text{HNO}_3\text{HNO}_3)^-$. The p-type electronic conduction suggests that electrons are withdrawn from graphite to form H^0 -like species.

Free protons in polyanilines or polypyrroles have been recently observed ([57] and F. Fillaux et al., unpublished). Polyanilines obtained from mild oxidation of aniline in acidic media are unusual members of the class of conducting polymers. Their electronic properties are not related to their conjugated carbon backbones in a simple way. Several derivatives with changes of electronic conductivity over 10 orders of magnitude can be obtained, depending upon the oxidation level, the protonation degree and the hydration state. The INS spectra of the emeraldine-base and salt and their ring-deuterated analogues evidence recoiling entities with mass $\sim 1 \text{ amu}$ [57]. The N–H band intensity is far too weak to be compatible with the sample stoichiometry. Most of the corresponding protons are delocalized and contribute to the continuum intensity. Free protons shed a new light onto the microscopic mechanisms that could determine electronic and protonic conductivities of these polymers. Similar conclusions can be drawn for polypyrroles (F. Fillaux et al., unpublished).

5. New protonic entities

5.1. $(\text{H}^+)_4$ in $\gamma\text{-MnO}_2$

The Mn^{4+} vacancies in $\gamma\text{-MnO}_2$ proposed by

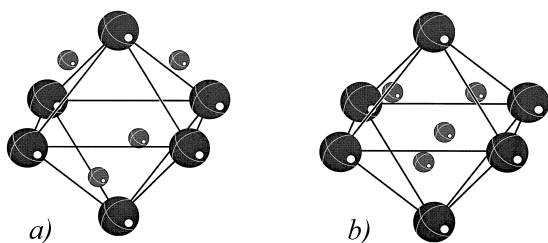


Fig. 12. Schematic view of the charge compensating protons (H^+)₄ associated with a Mn^{4+} vacancy in nsutite. (a) External configuration; (b) internal configuration.

Ruetschi [47] were supposed to be co-ordinated to four charge compensating protons which should play a major role as gateways between the structural channels for proton diffusion in three dimensions. Unfortunately, most of the experimental techniques (diffraction, NMR, QENS, infrared, Raman, etc.) are unable to provide direct information on the location and dynamics of these protons.

INS is unique to characterise charge compensating (H^+)₄ species [49–52]. The difference INS spectra obtained for various sample temperatures (e.g., 200–30 K in Fig. 11) are amenable to freely rotating spherical tops. This can be attributed to (H^+)₄ species with a tetrahedron structure at the centre of oxygen octahedra surrounding the Mn^{4+} vacancies. At low temperatures (e.g., 30 K) the charge compensating

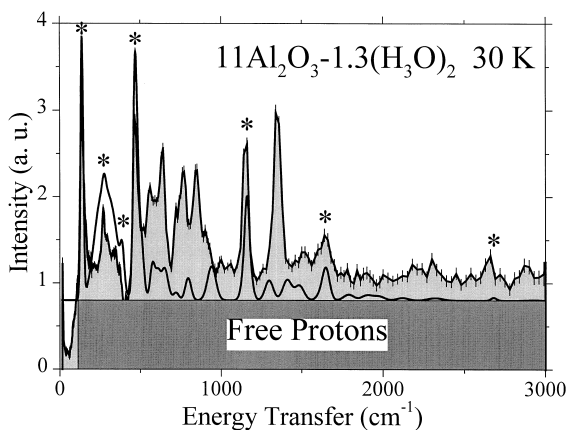


Fig. 13. Observed (with error bars) and calculated (for the tetrahedral structure of H_3O^+) INS spectra of β -alumina: (*) Band attributed to isolated H_3O^+ .

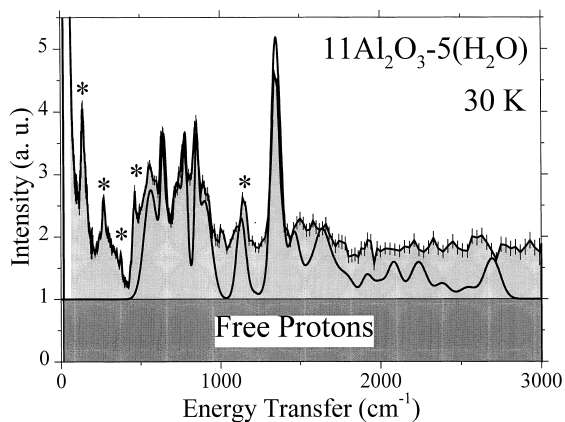


Fig. 14. Observed (with error bars) and calculated (for the tetrahedral structure of H_3O^+ perturbed by ion-ion interactions) INS spectra of β -alumina: (*) Band attributed to isolated H_3O^+ .

protons are outside the vacancies (Fig. 12(a)), and presumably contribute to the continuum intensity. As the temperature increases, these protons enter the vacancies to form freely rotating tetrahedron entities (Fig. 12(b)). The energy difference of $\sim 100\text{ cm}^{-1}$ between the two configurations is compatible with the gateway effect at room temperature. The rotational constant ($B = 25\text{ cm}^{-1}$) gives a radius of gyration (0.5 \AA) very similar to the Mn^{4+} radius (0.53 \AA). (H^+)₄ and Mn^{4+} species are virtually equivalent with regard to the local structure.

From the spectroscopy viewpoint, this is a unique example of tunnelling frequency ($\sim 40\text{ cm}^{-1}$) for the inversion of the tetrahedron structure through the unstable square planar configuration.

5.2. H_4O^{2+} in β -alumina

β -(or β'')-alumina is one of the first protonic conductors that has been studied with many techniques. The electrical conduction is purely ionic and is in two-dimension. Conduction mechanisms in terms of jump diffusion of oxonium (H_3O^+), hydroxonium ($H_5O_2^+$) or ammonium (NH_4^+) ions or protons have been proposed. Vibrational spectroscopy is necessary to characterise such disordered conducting entities. However, the spinel block matrix is opaque in the infrared region except above $\sim 1200\text{ cm}^{-1}$.

Therefore, only hydrogen bond free entities have been tentatively identified. With INS, the alumina matrix is virtually transparent and the vibrational dynamics of protonic entities can be observed over the whole spectral range. The high crystallinity of the host matrix and weak interactions between species inserted in the conducting planes yield well resolved spectra that can be analysed in detail with model force fields (Figs. 13 and 14).

The spectrum of the less hydrated sample $11\text{Al}_2\text{O}_3 \cdot 1.3(\text{H}_3\text{O})_2\text{O}$ is normally supposed to be dominated by nearly isolated H_3O^+ entities (Fig. 13). Surprisingly, the simulation did not confirm the C_{3v} or D_{3h} symmetry [58]. Instead, the spectral profile is amenable to a tetrahedral structure. However, it is quite unlikely that three protons could be delocalized over four sp^3 orbital in H_3O^+ . H_4O^{2+} entities with tetrahedral symmetry could be more in line with the strong acidity of β -alumina. The remarkable sharpness of the translational modes suggests these entities be trapped in well-defined sites. As there is no site symmetry related to T_d , the tetrahedron structure is not imposed by the environment. These entities are isomorphic to NH_4^+ , which are known to form regular networks in β'' -alumina, and can play almost identical roles.

The spectrum of the hydrated β -alumina $11\text{Al}_2\text{O}_3 \cdot 5\text{H}_2\text{O}$ is not amenable to hydroxonium entities H_5O_2^+ (Fig. 14). These entities are normally regarded as two water molecules linked by a rather strong hydrogen bond. They are supposed to be planar with a centre of symmetry. The INS spectrum is better represented with entities, still with T_d symmetry, whose translational and rotational degrees of freedom are shifted upwards, compared to the less hydrated sample. Presumably, the consequence of hydration is the formation of a dense packed layer of T_d entities perturbed by ion–ion interactions.

The continuum intensity in β -alumina reveals that free protons may also contribute to the conductivity. This continuum is very little affected by the hydration degree.

6. Conclusion

The full analysis of the INS vibrational spectra with the use of spectral intensities and momentum transfer

dependence provides a totally new view of quantum dynamics for proton transfer along hydrogen bonds. The double minimum potentials derived from vibrational spectra are quite different from those proposed from previous NMR and QENS works. Further, there is virtually no coupling of the proton dynamics with heavy atoms and the vibration assisted tunnelling model is not relevant.

The previous picture of hydrogen bonding in amides and polypeptides is seriously in error. The valence bond representation of the force field is not adequate. The proton stretching mode is at $\sim 1575 \text{ cm}^{-1}$ instead of $\sim 3300 \text{ cm}^{-1}$. The intense INS band observed at 40 cm^{-1} for polyglycine II is assigned to proton tunnelling in a symmetric double minimum potential. In the picture that can be extrapolated for amides and polyglycines at room temperature, hydrogen bonds form a network, with protons being delocalized between two virtually equivalent sites. The structure of the peptide unit is intermediate between amide-like and imidol-like structures. Proton transfer, an essential process in biology, is achieved naturally as a result of hydrogen bonding. Moreover, rather weak perturbations can localise the proton in one of the potential wells, favouring either amide-like or imidol-like structures.

Free protons are observed in many different systems and could play a key role in protonic conduction mechanisms. This discovery is still rather new and only the most straightforward consequences can be tentatively presented. The density of free protons is too small to give rise to measurable Fermi band structures. Free entities could be H^+ in $\gamma\text{-MnO}_2$ or coals, H^0 in HNO_3 intercalated graphite, or various mixtures of both in polyanilines. Unfortunately, the INS technique cannot determine effective charges. This strong limitation precludes a complete view of the subtle exchanges between free protons and electrons of the host. Complementary approaches are necessary.

Detailed characterisations of $(\text{H}^+)_4$ entities in $\gamma\text{-MnO}_2$, or of the tetrahedron structure of protonated water in β -alumina are also outstanding contributions to the mechanisms determining the electrochemical activity of these materials.

INS spectroscopy is still in its infancy. However, it reveals new fields of investigation for proton containing materials.

Acknowledgements

I would like to thank all colleagues who have contributed to this work and the ISIS pulsed neutron source for providing beam time and substantial technical support.

References

- [1] B. Fain, *Theory of Rate Processes in Condensed Media*, Springer, Berlin, 1960.
- [2] R.P. Bell, *The Proton in Chemistry*, Chapman and Hall, London, 1973.
- [3] R.P. Bell, *The Tunnel Effect in Chemistry*, Chapman and Hall, London, 1980.
- [4] R.P. Bell, *Special Issues Chem. Phys.* (1989) 135.
- [5] R.P. Bell, *Special Issues Chem. Phys.* (1993) 170.
- [6] V.A. Benderski, D.E. Makarov, C.A. Wight, *Chemical dynamics at low temperature*, in: I. Prigogine, S.A. Rice (Eds.), *Advances in Chemical Physics*, LXXXVIII, Wiley, New York, 1994.
- [7] Ph. Colombari Ed., *Proton Conductors, Solids, Membranes and Gels-Materials and Devices*, Cambridge University Press, Cambridge, 1992.
- [8] S.W. Lovesey, *Theory of Neutron Scattering from Condensed Matter*, Clarendon Press, Oxford, 1984.
- [9] E.B. Wilson Jr., J.C. Decius, P.C. Cross, *Molecular Vibrations*, McGraw-Hill, New York, 1995.
- [10] P. Barchewitz, *Spectroscopie Infrarouge*, Gauthier-Villars, Paris, 1967.
- [11] S.J. Cyvin, *Molecular Vibrations and Mean-Square Amplitudes*, Elsevier, Amsterdam, 1968.
- [12] A.I. Kitaigorodsky, *Molecular Crystals and Molecules*, Academic Press, New York, 1973.
- [13] S. Califano, V. Schettino, N. Neto, *Lattice Dynamics of Molecular Crystals*, Springer, Berlin, 1981.
- [14] A.J. Pertsin, A.I. Kitaigorodsky, *The Atom-Atom Potential Method*, Springer Series in Chemical Physics, Springer, Berlin, 1987.
- [15] A.C. Zemach, R.J. Glauber, *Phys. Rev.* 101 (1956) 118.
- [16] H. Jobic, J. Tomkinson, A. Renouprez, *Mol. Phys.* 39 (1980) 989.
- [17] H. Jobic, R.E. Gosh, A. Renouprez, *J. Chem. Phys.* 75 (1981) 4025.
- [18] A. Griffin, H. Jobic, *J. Chem. Phys.* 75 (1981) 5940.
- [19] H. Jobic, H. Lauter, *J. Chem. Phys.* 88 (1988) 5450.
- [20] G.J. Kearley, *J. Chem. Soc. Faraday Trans II* 82 (1986) 41.
- [21] F. Fillaux, J. Tomkinson, J. Penfold, *Chem. Phys.* 124 (1988) 425.
- [22] F. Fillaux, J.P. Fontaine, M.H. Baron, G.J. Kearley, J. Tomkinson, *Chem. Phys.* 176 (1993) 249.
- [23] F. Fillaux, J.P. Fontaine, M.H. Baron, N. Leygue, G.J. Kearley, *J. Tomkinson, Biophys. Chem.* 53 (1994) 155.
- [24] F. Fillaux, *Physica D* 113 (1998) 172.
- [25] G.J. Kearley, F. Fillaux, M.H. Baron, S. Bennington, J. Tomkinson, *Science* 264 (1994) 1285.
- [26] J.O. Thomas, R. Tellegren, I. Olovsson, *Acta Cryst. B* 30 (1974) 1155.
- [27] J.O. Thomas, R. Tellegren, I. Olovsson, *Acta Cryst. B* 30 (1974) 2540.
- [28] A. Novak, P. Saumagne, L.D.C. Bock, *J. Chim. Phys.* (1963) 1385.
- [29] K. Nakamoto, Y.A. Sarma, K. Ogoshi, *J. Chem. Phys.* 43 (1965) 1177.
- [30] G. Lucazeau, A. Novak, *J. Raman Spectrosc.* 1 (1973) 573.
- [31] P. Schuster, G. Zundel, C. Sandorfy, *The Hydrogen Bond. Recent Developments in Theory and Experiments*, 1–3, North-Holland, Amsterdam, 1976.
- [32] H. Ratajczak, W.J. Orville-Thomas Eds., *Molecular Interactions, I*, Wiley, New York, 1980.
- [33] F. Fillaux, *Chem. Phys.* 74 (1983) 405.
- [34] J.L. Skinner, H.P. Trommsdorff, *J. Chem. Phys.* 89 (1988) 897.
- [35] F. Fillaux, A. Lautié, J. Tomkinson, G.J. Kearley, *Chem. Phys.* 154 (1988) 135.
- [36] F. Fillaux, J. Tomkinson, *Chem. Phys.* 158 (1991) 113.
- [37] F. Fillaux, J. Tomkinson, *J. Mol. Struct.* 270 (1992) 339.
- [38] J.L. Katz, B. Post, *Acta Cryst.* 13 (1960) 624.
- [39] L. Pauling, *The Nature of the Chemical Bond*, Cornell University Press, Ithaca, New York, 1960.
- [40] B. Lotz, *J. Mol. Biol.* 87 (1974) 169.
- [41] G.N. Ramachandran, C. Ramakrishnan, C.M. Venkatachalam, in: G.N. Ramachandran (Ed.), *Conformation of Biopolymer*, 2, Academic Press, London, 1967, pp. 429.
- [42] F. Fillaux, M.H. Baron, J. Mayers, J. Tomkinson, *Chem. Phys. Lett.* 240 (1995) 114.
- [43] F. Fillaux, B. Nicolai, M.H. Baron, A. Lautié, J. Tomkinson, G.J. Kearley, *Ber. Bunsenges. Phys. Chem.* 102 (1998) 384.
- [44] M. Barthes, M. Ribet, in: S. Cusack, H. Büttner, M. Ferrand, P. Langan, P. Timmins (Eds.), *Adenine Press*, 1997, pp. 35.
- [45] S. Johnson, J. Eckert, M. Barthes, R. McMullan, M. Muller, *J. Phys. Chem.* 99 (1995) 16253.
- [46] F. Fillaux, H. Ouboumour, J. Tomkinson, L.T. Yu, *Chem. Phys.* 149 (1991) 459.
- [47] P. Ruetschi, *J. Electrochem. Soc.* 131 (1984) 2737.
- [48] F. Fillaux, S.M. Bennington, J. Tomkinson, L.T. Yu, *Chem. Phys.* 209 (1996) 111.
- [49] F. Fillaux, H. Ouboumour, C. Cachet, J. Tomkinson, G.J. Kearley, L.T. Yu, *Chem. Phys.* 164 (1992) 311.
- [50] F. Fillaux, C. Cachet, H. Ouboumour, J. Tomkinson, L.T. Yu, *J. Electrochem. Soc.* 140 (1993) 585.
- [51] F. Fillaux, H. Ouboumour, C. Cachet, J. Tomkinson, L.T. Yu, *J. Electrochem. Soc.* 140 (1993) 592.
- [52] F. Fillaux, C. Cachet, H. Ouboumour, J. Tomkinson, C. Lévy-Clément, L.T. Yu, *Prog. Batteries Battery Mater.* 12 (1993).
- [53] F. Fillaux, R. Papoular, A. Lautié, J. Tomkinson, *Carbon* 32 (1994) 1325.
- [54] F. Fillaux, R. Papoular, A. Lautié, J. Tomkinson, *Fuels* 74 (1995) 865.

- [55] F. Fillaux, R. Papoular, S.M. Bennington, J. Tomkinson, J. Non-Cryst. Solids 188 (1995) 161.
- [56] P. Albers, G. Prescher, K. Seibold, D.K. Ross, F. Fillaux, Carbon 34 (1996) 903.
- [57] F. Fillaux, N. Leygue, R. Baddour-Hadjean, S.F. Parker, Ph. Colomban, A. gruger, A. Régis, L.T. Yu, Chem. Phys. 216 (1997) 281.
- [58] Ph. Colomban, F. Fillaux, J. Tomkinson, G.J. Kearley, Solid State Ionics 77 (1995) 45.